ISSN 0025-6544, Mechanics of Solids, 2023, Vol. 58, No. 4, pp. 1202–1213. © Allerton Press, Inc., 2023.
ISSN 0025-6544, Mechanics of Solids, 2023. © Allerton Press, Inc., 2023.

A New Approach to the Combination of Load Interaction Effects and Damage Functions in Fatigue Life Prediction Based on Ductile Dissipation Energy

Yuan Liu[a,*] and Qiwen Xue[a,]**

[a]*School of Civil Engineering, Dalian Jiao Tong University, Liaoning Dalian, 116028 China*

**e-mail: 15640832511@163.com*

***e-mail: xueqiwen@djtu.edu.cn*

Received January 23, 2023; revised March 22, 2023; accepted May 2, 2023

Abstract—To address the failure of the toughness dissipation energy model to capture the effect of inter-load loading history factors on structural fatigue life under variable amplitude loading, in this paper, taking into account the interaction between loads, load order, and real-time damage, the ratio of stress amplitude between two adjacent levels and the real-time fatigue damage degree is introduced into the model calculation, and a new interaction factor related to the real-time fatigue damage function is established to obtain an improved nonlinear fatigue life prediction model. The predictive capability of the improved fatigue life prediction model is verified based on the test data of a variety of commonly used materials, such as 45 steel and aluminum alloy Al-2024-T42, under two-level and multi-level variable amplitude loading. According to the comparison analysis between the model-predicted data and the experimental data, it can be seen that the modified nonlinear fatigue life prediction model in this paper can effectively predict the remaining fatigue life for different materials under the multiple-level variable amplitude loading. Compared with other models, it is closer to the real experimental value. The data required in the model can be obtained from experiments without introducing additional parameters, which is more suitable for practical engineering.

Keywords: toughness dissipation energy, fatigue life prediction, interaction factor, interaction between loads, nonlinear fatigue accumulation damage

DOI: 10.3103/S0025654423600113

1. INTRODUCTION

Fatigue failure is a common form of failure of structures in rail vehicles, most of which are subjected to cyclic loading during operation, where variable amplitude loading is also an important form of loading on these structures. In engineering applications, structures under variable amplitude loads are susceptible to fatigue damage, which can reduce structural safety and even cause major traffic accidents. Hence, predicting the fatigue life of structures under variable amplitude loads is particularly important [1, 2]. But most of the fatigue life prediction methods are limited to the fatigue life of structures under constant amplitude loading, such as the stress-strain life method [3], stress field strength method [4], life method based on continuous damage mechanics [5], etc. For the fatigue life prediction under variable amplitude load, considering the principle of economy, the fatigue life data under constant amplitude load is often used to estimate and then applied in engineering [6].

In recent years, experts and scholars have researched the fatigue life prediction of structures under variable amplitude loads and proposed various fatigue life prediction methods. These methods can be summarized into two types: One is based on fatigue accumulation damage theory, and the other is based on fracture mechanics [7, 8]. The basic principle of the fatigue life prediction method based on cumulative damage theory is to convert the fatigue life data under constant amplitude loading into fatigue life data under variable amplitude loading to calculate, which can be divided into linear theory and nonlinear theory. In the linear theory, the most widely used is Miner's damage law. Although it has the advantages of simple form and simpler principles and rules when the model is calculated, the loads are independent of each other, failing to consider load interactions and ignoring the order of load loading [9]. This method considers that there is no correlation between the cumulative effect of damage and the course of load loading, and its prediction of fatigue life results often has a large gap with the real test value because most metal

materials show an extremely high degree of nonlinearity in describing the relationship between damage and cyclic loading. After the linear theory was proposed, many scholars at home and abroad proposed many nonlinear damage models [10]. These nonlinear damage models consider different aspects of fatigue damage from internal and external factors. The more typical ones are based on S-N damage curves, energy method, physical degradation properties of materials method, and continuous damage mechanics. These methods can take into account the loading history of variable amplitude loads to some extent, and the predictions are all the better than the linear damage model.

Although domestic and foreign scholars have made numerous contributions to nonlinear fatigue life prediction, the mechanisms responsible for these effects are still unclear. In recent years, some scholars have explained fatigue damage from the energy perspective, regarded fatigue damage as an irreversible energy loss process, and selected physical parameters related to energy dissipation as physical quantities to characterize the fatigue damage mechanism. Ye et al. proposed a ductile dissipation model based on applying the energy dissipation process to fatigue damage. It requires fewer parameters, has a simple form, and is widely used in fatigue life prediction of materials [11]. However, the model cannot consider the interaction between the loads, which makes its accuracy still has some gap compared with the experimental value. Many improved models for the toughness dissipation energy model followed; for example, Peng and Lu proposed a new, improved model that further improved the model's accuracy [12, 13]. However, the improved model only shows the interaction between the loads in the form of stress ratio and has not yet considered the influence of real-time damage and other factors. The related problems still need further in-depth study.

In this paper, based on the ductile dissipative energy model proposed by Ye, a new nonlinear fatigue life prediction model is established by constructing a new exponential function as the interaction factor using the adjacent stress amplitude ratio and the real-time fatigue damage function, which is modified for the interaction factor between adjacent loads. The new model will predict the fatigue life of different structural materials under multi-stage variable amplitude loading, compare with fatigue test data to verify feasibility and validity, and conduct a comparative analysis with the original model.

2. NONLINEAR FATIGUE CUMULATIVE DAMAGE FUNCTION BASED ON TOUGHNESS DISSIPATION ENERGY

According to Ref. [11], it is known that toughness is the most significant physical quantity that changes with fatigue damage when different materials are subjected to variable amplitude loads. In the fatigue failure process, the decay of Young's modulus and yield strength is due to the continuous sprouting and expansion of cracks under cyclic loading, which reduces the effective bearing area of the material; the decay of plastic properties is related to the continuous depletion of movable dislocations inside the material and the formation of dislocation barriers; the decay of toughness can comprehensively describe the degradation behavior of yield strength and plastic properties. The degradation behavior of material mechanical parameters in fatigue can be comprehensively described by the parameters' logarithmic toughness variation (dissipation). Ye et al. analyzed experimental toughness data for different structures under different degrees of fatigue damage. They established the fatigue damage variables of the toughness dissipation model:

$$D = 1 - \frac{U_{T(n)}}{U_{T0}}, \tag{2.1}$$

where U_{T0} is the material's toughness in its initial undamaged state; $U_{T(n)}$ is the material's residual toughness after loading cycles. The following equation can express the relationship between material toughness dissipation and the number of variable amplitude load actions:

$$U_{T(n)} = U_{T0} + \frac{U_{T0} - U_{T(N_f-1)}}{\ln N_f} \ln\left(1 - \frac{n}{N_f}\right). \tag{2.2}$$

Or write it as a function of the stress magnitude e_a and the number of stress cycles N:

$$U_{T(n)} = U_{T0} + \frac{U_{T0} - U_{T(N_f-1)}}{\ln \frac{1}{2}(e_a/e_f')^{\frac{1}{b}}} \ln\left[1 - 2\left(\frac{e_a}{e_f'}\right)^{-\frac{1}{b}} N\right], \tag{2.3}$$

where e_a is the stress amplitude under variable amplitude loading; N_f is the fatigue life. The relationship between the two can be drawn from the Basquin equation: $e_a = e_f'(2N_f)^b$, where e_f' and b are the experimental parameters related to fatigue strength.

The above equation can represent the energy absorbed by the structure under variable amplitude loading before fatigue fracture; after substituting Eq. (2.2) into Eq. (2.1), the cumulative damage model is obtained:

$$D = -\frac{D_{N_f-1}}{\ln N_f}\ln\left(1-\frac{n}{N_f}\right), \tag{2.4}$$

where D_{N_f-1} is the critical damage after N_{f-1} cycles at a certain stress level; D_{N_f-1} is related to the physical properties of the material and the stress magnitude when the critical damage state is reached, and the value of D_{N_f-1} is approximately equal to 1 through the analysis of the study by Ye et al.

Therefore, the cumulative damage model of Eq. (2.4) can be expressed as:

$$D \approx -\frac{1}{\ln N_f}\ln\left(1-\frac{n}{N_f}\right). \tag{2.5}$$

For this model, relevant fatigue test data have been verified and analyzed. The theoretical damage evolution curve obtained is in good agreement with the actual value, which shows the reasonableness of the cumulative damage model.

Using the fatigue equivalent damage principle and combining with Eq. (2.5), the model is used to predict the remaining fatigue life under two levels of loading:

$$\frac{n_2}{N_{f2}} = \left(1-\frac{n_1}{N_{f1}}\right)^{\frac{\ln N_{f2}}{\ln N_{f1}}}. \tag{2.6}$$

From Eq. (2.6), it can be obtained that the cumulative damage is less than 1 when loaded in the High-Low mode and greater than 1 when loaded in the Low-High mode, which is consistent with the objective loading law, indicating that the model can predict the effect of loading sequence on fatigue life under variable amplitude loading to a certain extent.

Equation (2.6) is extended to predict the remaining fatigue life of the structure under multi-stage loading:

$$\frac{n_i}{N_{fi}} = \left\langle \left\{ \left[\left(1-\frac{n_1}{N_{f1}}\right)^{\frac{\ln N_{f2}}{\ln N_{f1}}} - \frac{n_2}{N_{f2}} \right]^{\frac{\ln N_{f3}}{\ln N_{f2}}} - \frac{n_3}{N_{f3}} \right\}^{\frac{\ln N_{f4}}{\ln N_{f3}}} - \cdots - \frac{n_{i-1}}{N_{f(i-1)}} \right\rangle^{\frac{\ln N_{fi}}{\ln N_{f(i-1)}}}. \tag{2.7}$$

From Eq. (2.7), it can be seen that the nonlinear fatigue cumulative damage model based on ductile dissipation energy is simple in form and does not contain other superfluous physical parameters, which have a high value for practical engineering applications. But it fails to consider the influence of the interaction between the load levels on the fatigue life, which makes its prediction accuracy of the remaining fatigue life of the structure affected to a certain extent, and relevant corrections need to be made to this model.

3. MODIFIED NONLINEAR FATIGUE CUMULATIVE DAMAGE FUNCTION

In response to the failure of the above model to consider the influence of interactions between loads, some scholars have proposed that it can be described as a stress ratio of two adjacent levels, the size of which determines the degree of interaction. The above model is modified in the form of a stress factor ratio. Under the action of the secondary load, the relationship between the first two levels of damage can be obtained from the principle of equivalent damage as follows:

$$D(n_2') = D(n_1)^{\left(\frac{\sigma_2}{\sigma_1}\right)}, \tag{3.1}$$

where $n_2^{'}$ is based on the principle of equivalent damage, the stress is σ_1 under the action of n_1 times equivalent to the number of times the stress is σ_2 under the action.

Substituting Eq. (3.1) into Eq. (2.6) yields the equivalent damage cycle ratio under secondary loading:

$$\frac{n_{22}^{'}}{N_{f2}} = 1 - \left(\frac{1}{N_{f2}}\right)^{\left[-\frac{\ln\left(1-\frac{n_1}{N_{f1}}\right)}{\ln(N_{f1})}\right]^{\frac{\sigma_2}{\sigma_1}}}. \tag{3.2}$$

Then the remaining fatigue life under the two levels of the load is:

$$\left(\frac{n_2}{N_{f2}}\right)_{cp} = \left(\frac{1}{N_{f2}}\right)^{\left[-\frac{\ln\left(1-\frac{n_1}{N_{f1}}\right)}{\ln(N_{f1})}\right]^{\frac{\sigma_2}{\sigma_1}}}. \tag{3.3}$$

The fatigue life prediction model is derived from corresponding to the fatigue life under multi-level loading as:

$$\left(\frac{n_i}{N_{fi}}\right)_{cp} = \left(\frac{1}{N_{fi}}\right)^{\left[\frac{-\ln\left(\left(\frac{n_{i-1}}{N_{f(i-1)}}\right)_{cp}-\frac{n_{i-1}}{N_{f(i-1)}}\right)}{\ln N_{f(i-1)}}\right]^{\frac{\sigma_{i-2}}{\sigma_{i-1}}\times\frac{\sigma_i}{\sigma_{i-1}}}}. \tag{3.4}$$

The subscript *cp* denotes the model's fatigue life prediction under the corresponding stress level; σ_i is the corresponding stress amplitude under the *i* load level.

Although equation (3.1) has a certain improvement on the original model, the prediction accuracy has also been improved. Still, the model only considers the influence of the sequence of actions of the load, failing to consider the effect of fatigue damage on fatigue life corresponding to all stress levels under the action of variable amplitude load. Hence, the damage law for the fatigue accumulation model needs further study.

For variable amplitude loading action, the accumulated fatigue damage when reaching fatigue life is often not equal to 1. The accumulated damage value is less than 1 when loading from a high-stress level to a low-stress level, while the accumulated damage is often greater than 1 when loading from a low-stress level to a high-stress level [14]. This shows that the initial high stress prompted the crack generation. In contrast, the initial low stress had an exercise effect on the structure, so only taking the stress ratio cannot explain the interaction between the loading levels loading. So in this paper, a real-time damage function is introduced to reflect different stresses' roles on the structure.

According to the fatigue equivalence principle, the fatigue damage equation to cycle number ratio can be expressed in the form of some power function, such as the Manson model. To better describe the interaction, the interaction factor is defined in this paper as a function of the stress amplitude ratio combined with the real-time damage, i.e., described as:

$$\omega_{i-1,i} = \left(\frac{\sigma_i}{\sigma_{i-1}}\right)^{\exp(D_{i-1})}. \tag{3.5}$$

This results in a description of the remaining fatigue life fraction of the member under multi-level variable amplitude loading:

$$[F((n_{i-1}^{'} + n_{i-1})/N_{f(i-1)}, \sigma_{i-1})]^{\omega_{i-2,i-1}} = [F(1 - n_i/N_{fi}, \sigma_i)]^{\omega_{i-1,i}}, \tag{3.6}$$

where is the equivalent equation of state for fatigue damage, and $\omega_{I-1,i}$ is the interaction factor between loads of level $i-1$ and level i.

Based on the above analysis, combining Eq. (3.5) with Eq. (3.1) and Eq. (3.3) yields a modified nonlinear cumulative damage model under two-level loading, as shown in the following equation:

Table 1. Fatigue life prediction results of 45 steel using different models

Loading condition/MPa	Experimental data				Miner rule	Peng's model	Ye's Model	Modified model
	n_1	n_1/N_{f1}	n_2	n_2/N_{f2}				
331.5-284.4	500	0.0100	423700	0.8474	0.99	0.97	0.9879	0.96
	12500	0.2500	250400	0.5008	0.75	0.56	0.7055	0.55
	25000	0.5000	168300	0.3360	0.50	0.29	0.4314	0.28
	37500	0.7500	64500	0.1290	0.25	0.11	0.1861	0.10
284.4-331.5	125000	0.2500	37900	0.758	0.75	0.8810	0.7888	0.883
	250000	0.5000	38900	0.778	0.50	0.7040	0.5647	0.711
	375000	0.7500	43400	0.868	0.25	0.4549	0.3188	0.471

$$\left(\frac{n_2}{N_{f2}}\right)_{cp} = \left(\frac{1}{N_{f2}}\right)^{\left[\frac{\ln\left(1-\frac{n_1}{N_{f1}}\right)}{-\ln(N_{f1})}\right]^{\omega_{1,2}}}, \tag{3.7}$$

where, from Eq. (3.5), we get $\omega_{1,2} = \left(\frac{\sigma_2}{\sigma_1}\right)^{\exp(D_1)}$. Similarly, extending Eq. (3.7) to a multi-level load is:

$$\left(\frac{n_i}{N_{fi}}\right)_{cp} = \left(\frac{1}{N_{fi}}\right)^{\left[\frac{-\ln\left(\left(\frac{n_{i-1}}{N_{f(i-1)}}\right)_{cp}-\frac{n_{i-1}}{N_{f(i-1)}}\right)}{\ln N_{f(i-1)}}\right]^{\omega_{i-1,i}\times\omega_{i-2,i-1}}}. \tag{3.8}$$

Equation (3.8) is the proposed improved nonlinear fatigue damage model; the model contains both the interaction factor of the front and rear load ratios but also contains the real-time damage function; the form is simple, without the introduction of redundant parameters, not only to ensure that the load loading order, the influence of the interaction between the load, but also do not need to introduce other additional parameters, suitable for fatigue life prediction analysis in practical engineering.

4. EXAMPLE ANALYSIS

4.1. Fatigue Life Prediction Results under Two-Level Load

To verify the feasibility of the modified model proposed in this paper for fatigue life prediction, the remaining life prediction will be carried out based on the fatigue test data collected and compiled from the literature for the components, which are 45 steel, aluminum alloy Al-2024-T42, and 30CrMnSiA, respectively, and in the tests their loading methods were all stress-controlled with a stress ratio of $R = -1$. So that the prediction accuracy of the model can be better reflected, the prediction results of the modified model are compared with the Miner model and the original model, and the prediction results of Peng's improved model are compared and analyzed.

Example 1: Comparative analysis of fatigue life prediction results for 45 steel

Steel 45 is a common material in vehicle engineering and is often used in the processing and manufacturing parts for vehicles, etc., because of its good mechanical properties. According to the literature's secondary loading test of 45-gauge steel [15] as an example, the test value and the fatigue life prediction results of different models were compared and analyzed to get the error of each model for the actual measured value of the test data, which was used as a basis for comparative analysis. The specific test loading parameters and fatigue life prediction results and errors are shown in Tables 1 and 2 below, and comparative graphs of fatigue life are shown in Figs. 1 and 2 below.

Example 2: Comparative analysis of fatigue life prediction results for Aluminum alloy Al-2024-T42.

Aluminum alloy Al-2024-T42 is a high-strength material widely used in aerospace. It is often used to manufacture highly loaded components, such as aircraft skins and wings, because of its high strength and stability in high-temperature environments. According to the secondary loading test of aluminum alloy

Table 2. Fatigue life prediction results of 45 steel using different models

Loading Mode	Errors of different models			
	miner rule	Peng's model	Ye's model	modified model
1	16.83%	14.20%	16.58%	13.00%
2	49.76%	11.34%	40.87%	9.80%
3	48.54%	14.20%	28.16%	16.60%
4	93.80%	18.37%	44.26%	22.50%
5	1.06%	16.31%	4.06%	16.50%
6	35.73%	9.52%	27.42%	8.60%
7	71.20%	47.59%	63.27%	45.00%

Al-2024-T42 in the literature [16], for example, the fatigue life prediction results of different models are compared and analyzed to obtain the error of each model for the measured value of the test data, and this is used as a basis for comparison and analysis. The specific test loading parameters and fatigue life prediction results and errors are shown in Table 3 and 4 below. The comparison graphs of fatigue life prediction results and test values are shown in Figs. 1 and 2 below.

Example 3: Comparative analysis of fatigue life prediction results for 30CrMnSiA.

30CrMnSiA is a widely used wear-resistant material for bearings and gears, and it is often used in the manufacture of precision instruments because of its high strength and good wear resistance. According to the secondary loading test of 30CrMnSiA in literature [17] as an example, the fatigue life prediction results of different models were compared and analyzed to get the error of each model for the measured values of test data. The comparative analysis was carried out based on this. The specific test loading parameters and fatigue life prediction results and errors are shown in Tables 5 and 6 below. The comparison graphs of fatigue life prediction results and test values are shown in Figs. 1 and 2 below.

According to the above three arithmetic examples, the model in this paper is compared with the Miner model and Ye model for remaining fatigue life estimation. The errors with the measured values of test data are calculated respectively. The comparative analysis of the predicted and test values of the three models for different materials under the H-L loading sequence and L-H loading sequence is represented in Figs. 1 and 2. Analyzing Tables 1-6 above, it can be seen that the average errors are 45.3%, 68.0% and 51.8% using the Miner model, 32.1%, 61.0% and 36.1% using the Ye model, and 18.8%, 13.9% and 4.3% using the modified model of this paper, respectively, which are improved compared with the Miner model by 26.5%,

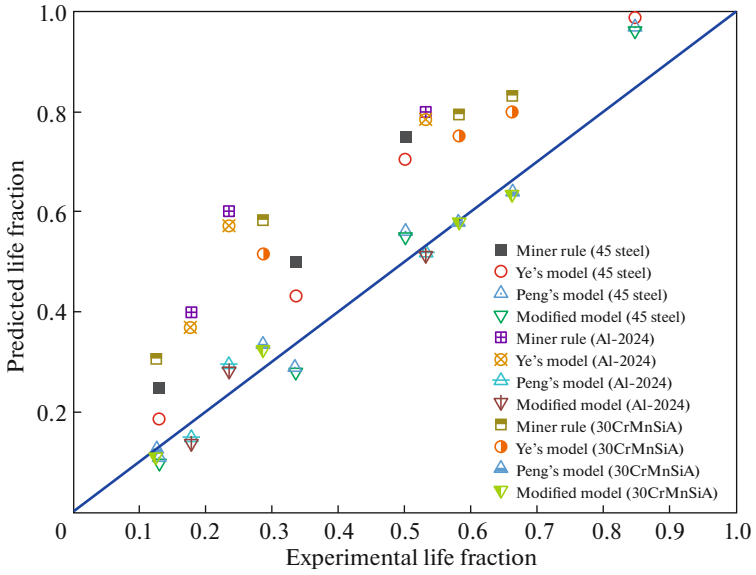

Fig. 1. Comparison between the experimental and predicted life fractions for welded joints under H–L loading sequences.

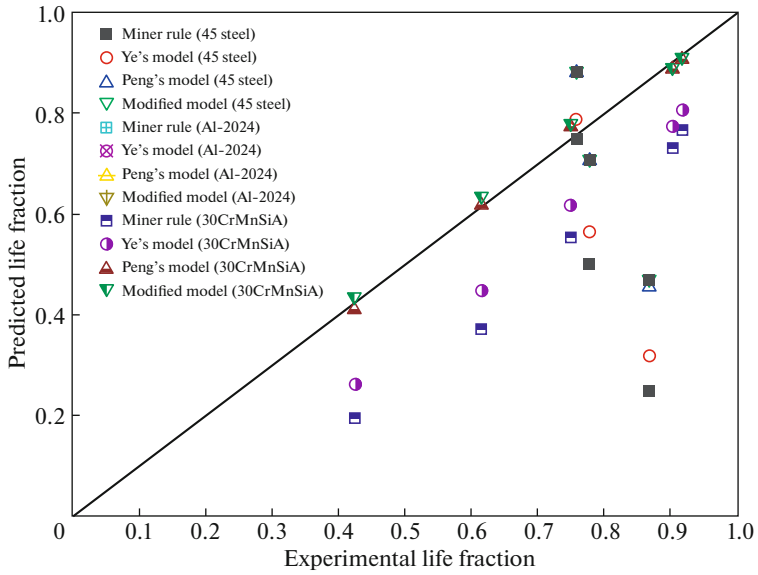

Fig. 2. Comparison between the experimental and predicted life fractions for welded joints under L–H loading sequences.

54.1%, and 47.5%, respectively, compared with the Miner model, and 13.3%, 47.1%, and 31.8%, respectively, compared with the original Ye model. Therefore, the model's prediction accuracy in this paper is slightly improved, which can be more effective for fatigue life prediction and has certain engineering practicality.

4.2. Fatigue Life Prediction Results under Multi-level Load

To further verify the feasibility and validity of the modified model in this paper under multi-stage loading, the fatigue test data of aluminum alloy 6082T6 under four-stage variable amplitude loading and the measured fatigue test data of 41Cr4 under five- and six-stage variable amplitude loading in the literature [18] are used in this section to compare the fatigue life prediction accuracy of Miner model, Ye model and the model in this paper for analytical verification. In the tests their loading methods were all stress-controlled with a stress ratio of R=-1.

Example 1: Comparison of fatigue life prediction results of aluminum alloy 6082T6 under four levels of loading.

The test value of the material and the fatigue life prediction results are compared and analyzed to get the error of each model for the actual measured value of the test data, based on which a comparative analysis is carried out, and the specific test loading parameters and fatigue life prediction results are shown in Table 7 below. The comparison graph between the fatigue life prediction results and the test value is shown in Fig. 3 below.

Example 2: Comparison of fatigue life prediction results of 41Cr4 under five levels of loading.

Table 3. Fatigue life prediction results of Aluminum alloy Al-2024-T42 using different models

Loading condition/MPa	Experimental data				Miner rule	Peng's model	Ye's model	Modified model
	n_1	n_1/N_{f1}	n_2	n_2/N_{f2}				
200–150	30000	0.2000	228700	0.5319	0.8	0.5186	0.7844	0.5130
	60000	0.4000	101050	0.2350	0.6	0.2947	0.5735	0.2840
	90000	0.6000	76050	0.1769	0.4	0.1505	0.3689	0.1380
150–200	86000	0.2000	144500	0.9633	0.8	0.9484	0.8146	0.9500
	172000	0.4000	133500	0.8900	0.6	0.8524	0.6254	0.8600
	258000	0.6000	81700	0.5447	0.4	0.7061	0.4309	0.7241

Table 4. Fatigue life prediction errors of Aluminum alloy Al-2024-T42 using different models

Loading mode	Errors of different models			
	miner rule	Peng's model	Ye's model	modified model
1	50.40%	2.50%	47.47%	3.50%
2	155.32%	25.40%	144.04%	20.80%
3	126.12%	14.92%	108.54%	21.80%
4	16.95%	1.55%	15.44%	1.38%
5	32.58%	4.22%	29.73%	3.37%
6	26.57%	29.63%	20.89%	32.80%

Table 5. Fatigue life prediction results of 30CrMnSiA using different models

Loading condition/MPa	Experimental data				Miner rule	Ye' model	Peng's model	Modified model
	n_1	n_1/N_{f1}	n_2	n_2/N_{f2}				
586–482	1200	0.1670	36911	0.662	0.833	0.7986	0.6389	0.6350
	1800	0.2080	32450	0.582	0.792	0.7505	0.5784	0.5789
	3000	0.4170	16002	0.287	0.583	0.5147	0.3357	0.3250
	5000	0.6940	6969	0.125	0.306	0.2328	0.1245	0.1130
482–586	13000	0.2330	6602	0.917	0.767	0.8061	0.9079	0.910
	15000	0.2690	6501	0.903	0.731	0.7752	0.8884	0.891
	25000	0.4480	5400	0.750	0.552	0.6171	0.7729	0.780
	35000	0.6280	4428	0.615	0.372	0.4478	0.6197	0.635
	45000	0.8070	3254	0.425	0.193	0.2627	0.4113	0.436

The test value of the material and the fatigue life prediction results are compared and analyzed to get the error of each model for the actual measured value of the test data, based on which a comparative analysis is carried out, and the specific test loading parameters and fatigue life prediction results are shown in Table 8 below. The comparison graph between the fatigue life prediction results and the test value is shown in Figure 4 below.

Example 3: Comparison of fatigue life prediction results of 41Cr4 under six levels of loading.

The test value of the material and the fatigue life prediction results are compared and analyzed to get the error of each model for the actual measured value of the test data, based on which a comparative analysis is carried out, and the specific test loading parameters and fatigue life prediction results are shown in

Table 6. Fatigue life prediction results of 30CrMnSiA using different models

Loading mode	Errors of different models			
	miner rule	Peng's model	Ye's model	Modified model
1	25.83%	3.49%	20.63%	4.00%
2	36.08%	0.62%	28.95%	0.50%
3	103.14%	16.97%	79.34%	13.40%
4	144.80%	0.40%	86.24%	9.60%
5	16.36%	0.99%	12.09%	0.80%
6	19.05%	1.62%	14.15%	1.30%
7	26.40%	3.05%	17.72%	4.10%
8	39.51%	0.76%	27.19%	3.30%
9	54.59%	3.22%	38.19%	2.50%

Table 7. Fatigue life prediction results of aluminum alloy 6082T6 using different models

Stress level	Stress amplitude/MPa	Experimental data			Miner rule		Ye's model		Modified model	
		n_i	N_{fi}	n_i/N_{fi}	n_4/N_{f4}	REP	n_4/N_{f4}	REP	n_4/N_{f4}	REP
1	305	10950	38000	0.29	0.3400	159.24%	0.2800	111.54%	0.2100	61.53%
2	280	19427	87612	0.22						
3	260	26258	180660	0.14						
4	240	52500	394765	0.13						

Table 8. Fatigue life prediction results of 41Cr4 under five levels using different models

Stress level	Stress amplitude/MPa	Experimental data			Miner rule		Ye's model		Modified model	
		n_i	N_{fi}	n_i/N_{fi}	n_5/N_{f5}	REP	n_5/N_{f5}	REP	n_5/N_{f5}	REP
1	350	44	56000	0.0008	0.7333	108.32%	0.7028	99.70%	0.6088	72.95%
2	332	352	74000	0.0048						
3	298	6160	130000	0.0474						
4	254	59840	280000	0.2137						
5	201	440000	1250000	0.3520						

Table 9 below. The comparison graph between the fatigue life prediction results and the test value is shown in Figure 5 below.

From the analysis of the calculation results and error results in Table 7–9 and Figs. 3–5 above, it can be seen that for both materials of aluminum alloy 6082T6 specimen and 41Cr4 specimen under multi-stage variable amplitude load, the nonlinear fatigue life prediction correction model proposed in this paper can play an effective prediction role, and compared with the results calculated by Miner's law model and Ye model, the calculation accuracy is improved by 97.71%, 35.37%, 94.28% and 50.01%, 26.75%, 65.20%, making the prediction results closer to the test values, and the greater the degree of real-time damage, the more significant the effect of interaction factors.

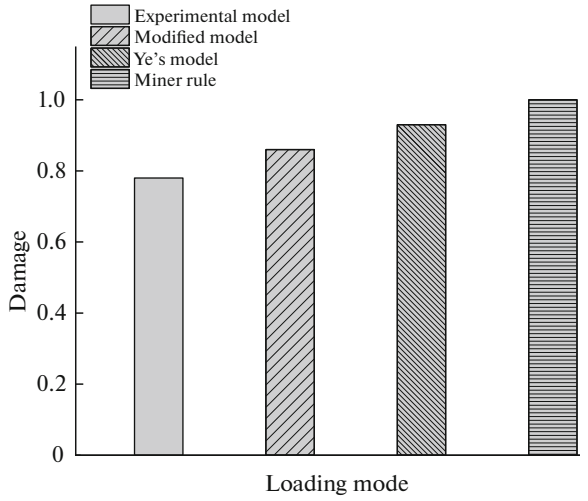

Fig. 3. Comparison of fatigue damage results of aluminum alloy 6082T6 specimens under 5 levels of loading.

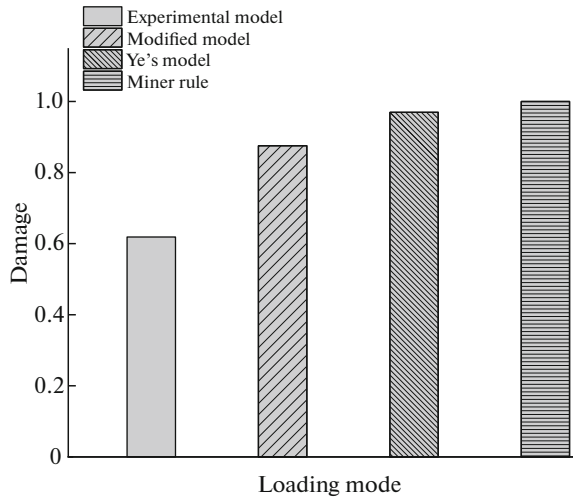

Fig. 4. Comparison of fatigue damage results of 41Cr4 specimens under 5 levels of loading.

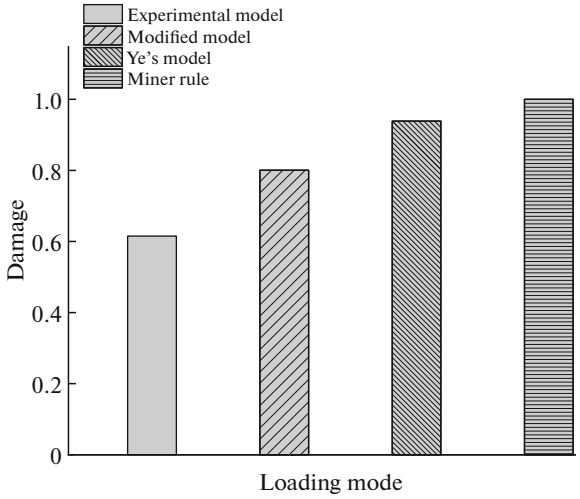

Fig. 5. Comparison of fatigue damage results of 41Cr4 specimens under 6 levels of loading.

Table 9. Fatigue life prediction results of 41Cr4 under six levels using different models

Stress level	Stress amplitude/MPa	Experimental data			Miner rule		Ye's model		Modified model	
		n_i	N_{fi}	n_i/N_{fi}	n_6/N_{f6}	REP	n_6/N_{f6}	REP	n_6/N_{f6}	REP
1	505	4	9000	0.0004	0.5963	181.94%	0.5348	152.86%	0.3969	87.66%
2	475	32	11600	0.0028						
3	423	560	21000	0.0267						
4	362	5440	47000	0.1157						
5	287	40000	155000	0.2581						
6	212	184000	870000	0.2115						

5. CONCLUSIONS

1. A feasible fatigue life prediction model is constructed to establish a new interaction factor by combining the real-time damage state parameters of variable amplitude loads with the adjacent stress amplitude ratio. The improved prediction model can not only better consider the effect of interaction between variable amplitude loads, but also effectively deal with the effect of variable amplitude load interaction on fatigue damage accumulation of different materials.

2. According to the fatigue life comparison results for different materials, the ability of the improved model to predict fatigue life under variable amplitude load of secondary load or even multi-level load is improved to a certain extent, and the prediction analysis results are closer to the real test results than the original model and Miner's rule.

3. The improved nonlinear fatigue life prediction model is simple in form, clear in the physical meaning, and does not need to introduce additional physical parameters. The required parameters can be obtained experimentally and better characterize the fatigue damage evolution, which is very suitable for the fatigue life prediction of actual engineering structures.

FUNDING

This study was supported by the Natural Science Foundation of Liaoning Province (no. 2019KF0204); and Liaoning Province 2020 College Innovation Talents Support Plan

REFERENCES

1. R. Kashyzadeh, Kazem, et al. "Fatigue life analysis of automotive cast iron knuckle under constant and variable amplitude loading conditions," Adv. Appl. Mech. **3** (2), 517–532 (2022). https://doi.org/10.3390/applmech3020030
2. J. Papuga, M. Margetin, and V. Chmelko, "Various parameters of the multiaxial variable amplitude loading and their effect on fatigue life and fatigue life computation," Fatigue Fract. Eng. Mater. Struct. **44** (10), 2890–2912 (2021). https://doi.org/10.1111/ffe.13560
3. M. Nihei, P. Heuler, Ch. Boller, and T. Seeger, "Evaluation of mean stress effect on fatigue life by use of damage parameters," Int. J. Fatigue **8** (3), 119–126 (1986). https://doi.org/10.1016/0142-1123(86)90002-2
4. W. X. Yao, "The description for fatigue behaviours of metals by stress field intensity approach," J. Solid Mech. **18**, 38–48 (1997). https://doi.org/10.19636/j.cnki.cjsm42-1250/o3.1997.01.005
5. J. L. Chaboche, and P. M. Lesne, "A non-linear continuous fatigue damage model," Fatigue Fract. Eng. Mater. Struct. **11** (1), 1–17 (1988). https://doi.org/10.1111/j.1460-2695.1988.tb01216.x
6. M. Domaneschi, et al. "Collapse analysis of the Polcevera viaduct by the applied element method," Eng. Struct. **214**, 110659 (2020). https://doi.org/10.1016/j.engstruct.2020.110659
7. P. Paris and F. Erdogan, "A critical analysis of crack propagation laws," J. Basic Eng. **85** (4), 528–533 (1963). https://doi.org/10.1115/1.3656900
8. X. H. Yang, W. X. Yao, and C. M. Duan, "The review of ascertainable fatigue cumulative damage rule," Eng. Sci. **5** (4), 82–87 (2003). https://doi.org/10.3969/j.issn.1009-1742.2003.04.013
9. M. A. Miner, "Cumulative damage in fatigue," J. Appl. Mech. **12** (3), A159–A164 (1945). https://doi.org/10.1115/1.4009458
10. K. Gao and X. Gao, "Nonlinear fatigue reliability analysis based on improved toughness exhaustion damage," J. Railw. Sci. Eng. **19** (3), 807–813 (2022). https://doi.org/10.19713/j.cnki.43-1423/u.t20210237
11. D. Y. Ye and Z. L. Wang, "A new approach to low-cycle fatigue damage based on exhaustion of static toughness and dissipation of cyclic plastic strain energy during fatigue," Int. J. Fatigue **23** (8), 679–687 (2001). https://doi.org/10.1016/S0142-1123(01)00027-5
12. Z. Peng, H. Z. Huang, H. K. Wang, et al. "A new approach to the investigation of load interaction effects and its application in residual fatigue life prediction," Int. J. Damage Mech. **25** (5), 672–690 (2016). https://doi.org/10.1177/1056789515620910
13. W. Lu, W.B. You, S.G. Hu, et al. "Research on improved model of life assessment of missile recorder," J. Ordnance Equip. Eng. **41** (3), 136–140 (2020). https://doi.org/10.11809 /bqzbgcxb2020.03.027

14. L. Y. Xie, "On the equivalence of fatigue damage stress," J. Mech. Strength. **2**, 100–104 (1995). https://doi.org/10.16579/j.issn.1001.9669.1995.02.018
15. D. G. Shang and W. X. Yao, "Study on nonlinear continuous damage cumulative model for uniaxial fatigue," Chin. J. Aeronaut. **6**, 8–17 (1998). https://doi.org/10.3321/j.issn:1000-6893.1998.06.002
16. D. G. Pavlou, "A phenomenological fatigue damage accumulation rule based on hardness increasing, for the 2024-T42 aluminum," Eng. Struct. **24** (11), 1363–1368 (2002). https://doi.org/10.1016/S0141-0296(02)00055-X
17. Y. Q. Fang, M. M. Hu, and Y. L. Luo, "New continuous fatigue damage model based on whole damage field measurements," Chin. J. Mech. Strength. **28** (4), 582–596 (2006). https://doi.org/10.16579/j.issn.1001.9669.2006.04.023
18. A.D. Yu, et al. "A modified nonlinear fatigue damage accumulation model for life prediction of rolling bearing under variable loading conditions," Fatigue Fract. Eng. Mater. Struct. **45** (3), 852–864 (2022). https://doi.org/10.1111/ffe.13641